

Phase transformations in one-dimensional materials: applications in electronics and energy sciences

David T. Schoen,^a Stefan Meister,^a Hailin Peng,^a Candace Chan,^b Yuan Yang^b and Yi Cui^a

Received 18th November 2008, Accepted 13th March 2009

First published as an Advance Article on the web 27th April 2009

DOI: 10.1039/b820624d

Phase transformations at the nanoscale display interesting and important differences from those which occur in the bulk of most materials systems. These differences occur in a large variety of transformations, including melting, solid state phase transformation, chemical ordering and disordering, and chemical and electrochemical transformations. They arise from both the thermodynamic contribution of surface energy as well as the kinetic influence of small diffusion distances. These changes in the energetics and dynamics of transformation can prove important for a variety of technologies, including energy storage, energy conversion, and information technologies.

Introduction

Phase transformations in nanoscale materials are an important and timely subject of investigation. They are important from a fundamental perspective because the materials themselves are on the size scale of the smallest units of structural transformation, namely the nuclei and defects which dominate the early stages of most transformation processes. They display many important kinetic and thermodynamic differences from bulk materials due to the large and significant portion of their atoms which occupy surface sites. For these reasons they display a set of unique and sometimes tunable behaviors, which is an advantage for the rational design of a wide variety of technologies, several of which will be discussed in this feature article:

nonvolatile memory, energy storage and energy conversion. A great deal of work, both theoretical and experimental, has been completed in this area studying several types of transformations in a wide variety of materials systems. To date, the vast majority of this work has focused on zero-dimensional (0D) systems, namely those that have nanoscale dimensions in all three directions. The most important types of transformations studied so far are melting,^{1–3} solid state transitions induced by hydrostatic pressure,⁴ chemical transformations induced primarily through chemical or ion exchange reactions,⁵ and electrochemical transformations.^{6,7}

The most exciting next step to this body of research is to extend the findings on 0D systems, mostly nanocrystals, to 1-dimensional systems, nanowires. Like nanocrystals, nanowires also have a large fraction of surface atoms so display many important differences in their phase transformations from bulk materials. They have the added advantage that they can be easily integrated into working electrical devices, so many of these unique properties can be utilized in new and often surprising ways.

^aDepartment of Materials Science and Engineering, Stanford University, Stanford, CA, USA; Fax: +1 650 725 4034; Tel: +1 650 724 6256

^bDepartment of Chemistry, Stanford University, Stanford, CA, USA; Fax: +1 650 723 2501; Tel: +1 650 724 6256



David T. Schoen

David Schoen was born in Kentucky and received his B.S. in materials science from the Massachusetts Institute of Technology in 2005. He is currently pursuing his Ph.D. in Stanford University's materials science and engineering program. His focus is the synthesis and characterization of a wide variety of nano-materials, as well as the fabrication of single nanowire devices for in-situ transmission electron microscopy. He is a proud



Stefan Meister

Stefan Meister was born in Dortmund, Germany. He obtained a B.S. in physics from the University of Maine in 2005 and is currently pursuing a Ph.D. in materials science at Stanford University. His research interests include in situ TEM observation of phase changes in nano-structured materials.

recipient of the National Science Foundation Graduate Research Fellowship, the National Defense Science and Engineering Graduate fellowship, and the Stanford Graduate Fellowship.

The difference in dimensionality they afford will also provide a means to further assess much of the theoretical work which has been completed for nanocrystals. One-dimensional systems also provide an opportunity to study in a relatively simple geometry the movement of boundaries between transformed and untransformed domains, which is often impossible in nanocrystals since they usually transform in one coherent whole.⁴

Many topics of great interest in this area will not be taken up by this feature article, given the limited space available. A variety of interesting one-dimensional structures have been reported in the literature, including helical,^{8,9} branched,¹⁰ and hollow structures. Hollow 1D structures, or nanotubes, are the subject of a great deal of current research; interested readers are directed to other sources¹¹ for information on them. This feature article will focus on transformations driven by structural, chemical, and electrochemical forces, and will exclude work on ferroelectric^{12,13} and magnetic transformations.¹⁴ The numerous thermodynamic and kinetic phenomena which arise during nanostructure

synthesis will likewise be excluded, as good reviews^{15–17} on this topic are readily available.

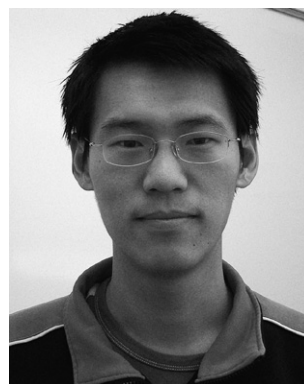
0D systems

The investigation of nanoscale phase transformation has a long history. The effect of diameter on the melting of small particles was considered theoretically as early as 1909,¹⁸ and some experiments were undertaken as early as 1959.¹⁹ Much of the initial work on this problem utilized electron diffraction on thin discontinuous metal films evaporated onto thin carbon membranes.¹² Through careful analysis of the data collected it was possible to verify that very small particles of a given material do have a lower melting point than the bulk value. This melting point depression is due to a relative lowering of the free energy of a liquid drop due to the lower surface energy of a material in its liquid rather than solid state. Fig. 1 shows the diameter



Hailin Peng

Hailin Peng was born in Hunan, China. He received his B.S. in chemistry from Jilin University in 2000 and a Ph.D. in physical chemistry from Peking University in 2005, working under the guidance of Professor Zhongfan Liu on nanochemistry and scanning tunneling microscopy. He pursued postdoctoral studies on nanomaterials science and engineering with Professor Yi Cui at Stanford University during 2005–2009. He became an Associate Professor in the College of Chemistry at Peking University in 2009.



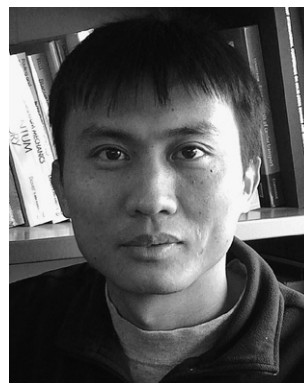
Yuan Yang

Yuan Yang completed his B.S. degree in the Department of Physics at Peking University in 2007, and Master's degree in materials science at Stanford University in 2009. He is currently a Ph.D. candidate in Prof. Yi Cui's group at Stanford University. His research topics focus on synthesis and properties of nanomaterials for lithium-ion battery cathodes. He is also interested in physical properties of various nanomaterials and nanodevices.



Candace Chan

A Texas native, Candace Chan attended Rice University, where she worked in Nobel Laureate Rick Smalley's group and received a B.S. in chemistry. After several internships at Los Alamos National Lab and Lawrence Berkeley National Lab, she went to Stanford to pursue a Ph.D. in physical chemistry. She is currently finishing her Ph.D. in Prof. Yi Cui's group in the materials science department at Stanford, where she is studying the use of nanomaterials as lithium-ion battery and supercapacitor electrodes. She was awarded the Paul J. Flory award for Physical Chemistry, the Stanford Graduate Fellowship, the NSF Graduate Fellowship, and the Miller Research Fellowship.



Yi Cui

Yi Cui got his Bachelor degree in chemistry at University of Science and Technology of China in 1998 and Ph.D. in chemistry at Harvard University in 2002. He went on to work as a Miller Postdoctoral Fellow at University of California, Berkeley. Since 2005, he has been an Assistant Professor in the Department of Materials Science and Engineering at Stanford University. He leads a group of researchers working on nanomaterials for energy, electronics and biotechnology. He has received the KAUST Investigator Award (2008), the ONR Young Investigator Award (2008), the MDV Innovators Award (2007) and the Technology Review World Top Young Innovator Award (2004).

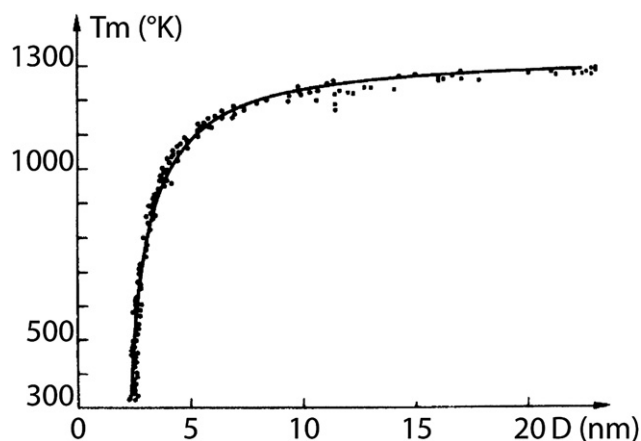


Fig. 1 Melting point vs. diameter in Au nanoparticles. From Buffat 1976.¹

dependence of gold particles vs. their diameter. The depression of melting point can be captured with a simple equation:¹⁸

$$T_b - T_m = \frac{2T_b}{L\rho_{sol}R_{sol}} \left[\gamma_{sol} - \gamma_{liq} \left(\frac{\rho_{sol}}{\rho_{liq}} \right)^{\frac{2}{3}} \right] \quad (1)$$

The change in melting point from the bulk value T_b to the new value for a given particle T_m depends on the latent heat of fusion L , the densities of the solid and liquid phases ρ_{sol} and ρ_{liq} , the radius of the particle R_{sol} and most importantly the surface energies of the solid and liquid phases γ_{sol} and γ_{liq} . The early work with metals has been extended into other classes of materials as well, with the same basic results.³ Solid state transformations have also been extensively studied. The most recent work in this area has focused on investigating structural changes in colloidal nanoparticles of various materials in a diamond anvil cell.^{21–25} This approach is very versatile since a large number of experimental techniques can be used, including Raman spectroscopy, optical adsorption, and various synchrotron X-ray techniques. A wide variety of materials have been investigated. Solid state transformations can also be modeled thermodynamically,²⁶ although the effects of both surface energy and surface stress must be included. Interestingly, in all these cases the transition pressure from the low pressure case to the high pressure case is elevated, not depressed as in the case of melting, indicating that in all these cases the higher pressure phase has a higher surface energy than the low pressure phase. This is not an expected result, but can be justified when one considers the mechanics of the phase transformation.²⁵ In nanocrystals, unlike bulk materials, each nanocrystal generally transforms as a coherent whole, without forming any internal boundaries or defects. This is accomplished through a cooperative movement of atoms along well defined transition paths. When the details of such paths are considered, it becomes plausible that the high pressure phases of the nanocrystals after transformation have a higher proportion of high energy facets, corners and edges than the initial nanoparticles grown often at elevated temperatures with a minimized surface energy for their size.

The ability of nanocrystals to undergo solid state transformations without forming internal defects or domains leads to

particularly interesting behavior during chemical transformations. Unlike bulk materials, they are small compared to reasonable diffusion distances at room temperature, and so can transform quickly even at ambient conditions.⁵ It is often possible to fully and reversibly interconvert materials through chemical reaction or ion exchange. Even when defects are formed during transformation, they often form interesting and unanticipated structures. For example, at the nanoscale, the Kirkendall effect, which leads to void formation in bulk diffusion couples, can be used in a variety of systems to make high quality hollow nanostructures.²⁷

1D nanostructures

One-dimensional nanostructures have received a great amount of interest for their potential application to a staggering number of technologies, including nanoelectronics,^{28–31} optics,³² biosensors,³³ and many types of energy storage and conversion including photovoltaics,^{34,35} thermoelectrics,^{36,37} nanogenerators,³⁸ and batteries.³⁹ In nearly all of these applications, the materials involved must undergo phase transformations during their synthesis or device processing, be stable at their operating conditions, or in some cases undergo repeated phase transformations as a fundamental part of their operation. For example, during vapor-liquid-solid (VLS) growth of nanowires, a nanoscale liquid metal droplet, which functions as a catalyst to nucleate and grow one-dimensional nanowires, is an interesting nanoscale system for studying phase transformation thermodynamics and kinetics. The study of phase transformation in these systems is for this reason critical for their successful use in the various technologies listed. In many cases the modified phase transformation behavior of nanoscale systems itself offers advantages over the same materials in the bulk, but in all cases this behavior must be understood.

One-dimensional systems also offer some advantages for fundamental study over zero-dimensional ones. The already mentioned ease of integration allows for the ability to study the behavior of individual nanostructures rather than their ensembles, for instance in phase change memory applications.^{40–42} Nanowires may also be placed under a more complicated set of strain conditions than the hydrostatic pressure widely investigated in nanocrystals, which can lead to unexpected structures and behaviors.⁴³ Unlike nanocrystals, which usually transform as a coherent whole, nanowires often transform in discrete domains. Unlike the bulk, this domain creation can be sustained in nanowires without fracturing or large scale morphological change, so the process of domain growth and boundary motion can be more easily studied,⁴⁴ and like nanocrystals, nanowires can often start and end a transformation process in single crystalline states.

The synthesis of high quality single crystal nanowires, although improving quickly, has not yet reached the level of flexibility and control available for nanocrystals. For this reason, many measurements carried out in nanocrystals as a function of size are still difficult to execute in nanowires, due to the requirements of sample size and homogeneity imposed by bulk measurement techniques. For this reason, the study of individual nanowires, especially by in-situ TEM techniques,^{20,45,46} is a common approach. This can be especially important in

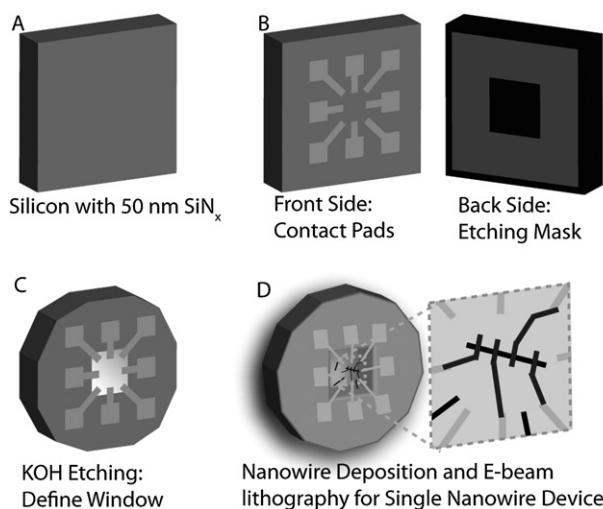


Fig. 2 In-situ single nanowire device fabrication. A) The process begins with a double side polished silicon wafer coated with a low stress 50 nm silicon rich silicon nitride film. B) Photolithography is used with lift-off processing to deposit gold contact pads on the front of the wafer, and with plasma etching to pattern the silicon nitride forming an etching mask on the back of the wafer. C) KOH etching is used to remove the silicon from behind the window area and to release individual windows for inserting into the TEM specimen holder. D)²⁰ Nanowires are randomly deposited onto the windows with one of a variety of processes and then e-beam lithography and lift-off is used to define metal contacts, forming single nanowire devices.

anisotropic materials in which a single synthesis may produce a collection of nanowires with more than one growth direction. As in the study of nanocrystals, developing a complete understanding of a materials system requires a large set of combined techniques. TEM can afford excellent structure and composition characterization. When combined with electron beam lithography to make single nanowire electrical devices it can directly demonstrate surprising correlations. We have developed this combined technique in our research group to study a set of phase transformation phenomena in nanowires. Fig. 2 outlines the fabrication process. Individual nanowires are located in relation to some prefabricated reference features on a silicon nitride window. Electron beam lithography and lift-off processing is used to define metal contacts to these nanowires. Once contact is made, electrical characterization and structural characterization with the TEM becomes possible, allowing for an unambiguous correlation between electrical properties and atomic structure.

An interesting example of the power of a combined experimental approach is the case of In_2Se_3 nanowires from our research group.²⁰ In_2Se_3 has a highly anisotropic crystal structure composed of covalently bound sheets of In-Se held together by much weaker van der Waals bonding. Fig. 3 illustrates the crystal structure and presents TEM data on nanowires in two different growth directions, $[11-20]$ nanowires with their growth direction parallel to the sheets, and $[0001]$ nanowires with their long axis perpendicular to the sheets. Nanowires of both types co-exist on the same substrate after synthesis. Single nanowire electrical devices would give two types of distinct electron transport behaviors but could not unambiguously identify the structural

origin of the difference of their electrical properties. When single nanowire devices are fabricated on top of a 50 nm thick SiN_x membrane, it is possible to correlate directly the structure of individual nanowires with their electrical properties. Excitingly, we found nanowires with the $[11-20]$ growth direction are metallic while nanowires with the $[0001]$ direction are semi-conducting. The conductivity ratio of $[11-20]$ to $[0001]$ direction can be up to 10^6 , which is 1–3 orders of magnitude larger than the bulk value.

Structural phase transformations in 1D

The transformations which have been most carefully studied in nanocrystals, namely melting and pressure induced solid state transformation, have also been investigated in one-dimensional structures, although much less extensively and with somewhat less rigor. The case of melting has been considered for Zn nanowires of various diameters grown in anodized alumina templates studied by differential scanning calorimetry.⁴⁷ As in the nanocrystal case, the melting point was found to be depressed with decreasing diameter, although there was some disagreement as to the interpretation of the experiment.^{48,49} Pd^{50} nanowires grown in mesoporous structures have been cursorily examined with in-situ TEM heating and have also exhibited a melting point depression, although only for isolated diameters so there is no information on the trend. In fact, since melting was demonstrated *via* morphological change in the nanowires rather than electron diffraction, there is some question as to the validity of the temperatures obtained. Melting in one-dimensional systems can be complicated by Raleigh instabilities,⁵¹ in which a cylindrical system can spontaneously decompose into a line of spheres. This process is driven by the need to reduce the surface energy of these systems, the same force which depresses the melting point. For this reason it is often more profitable to study other solid state transformations, such as order-disorder transitions, which generally take place without large morphological changes.

We can again consider the example of In_2Se_3 nanowires.⁵² As previously mentioned, In_2Se_3 has a structure composed of layers of covalently bound In-Se sheets van der Waals bonded to each other. Within these sheets, there are “vacant” indium sites. When these layers come together in a large crystal it is possible for these vacant sites to form ordered structures, generating a superlattice which is evident from electron diffraction (Fig. 4A). Such superlattices can be observed for both orientations of In_2Se_3 nanowires. The ordered structure is stable from room temperature to 200 °C in nanowires, at which point chemical disordering eliminates the superlattice (Fig. 4B). As in many of the other solid state transformations a significant hysteresis in the transformation was reported. After transformation the high temperature disordered structure was preserved all the way down to room temperature and persisted for at least several hours before reordering back to superlattices (Fig. 4C). Unlike in bulk materials with a reported superlattice stability range of 60 to 200 °C,⁵³ the superlattice structure is stable in nanowires at room temperature.

Another interesting set of systems in which to consider solid state transformations are the copper and silver chalcogenides. Many of these systems, such as Cu_2S and Ag_2Se , have a high

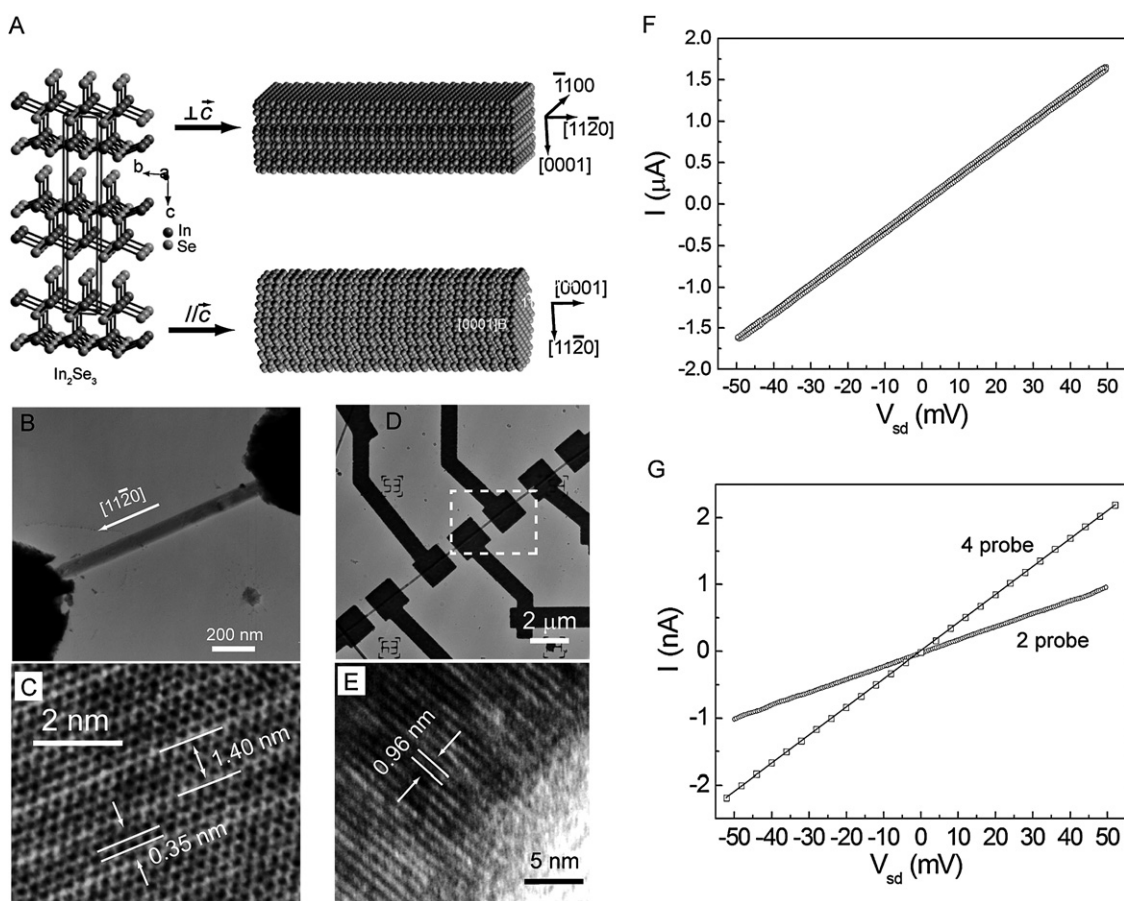


Fig. 3 (Ref. 20) A) Layered crystal structure of bulk In_2Se_3 based on the tetrahedral bonding of the Se-In-Se-In-Se layers and the two observed nanowire growth directions. B) TEM image of a $[11\bar{2}0]$ single nanowire device. C) HRTEM image of the device in B. D) TEM image of a $[0001]$ single nanowire device. E) HRTEM image of the device in E. F) I–V curve of the device in B. G) I–V curve of the device in E, with 2 and 4 probe measurements.

temperature super ionic phase, in which the mobility of the cations approaches or exceeds that of these materials in their liquid state.⁵⁴ This situation can be successfully modeled as a cationic liquid inside a solid anion lattice. This cationic melting can be observed by electron diffraction. This transformation displays very interesting behavior in one-dimensional nanoscale systems.

Fig. 5 shows our results of such an experiment for Ag_2Se nanowires synthesized in a two-step process.⁵⁵ First selenium nanowires are grown *via* directional Ostwald ripening of trigonal selenium nuclei.⁵⁶ These selenium nanowires can then be fully converted to single crystal Ag_2Se nanowires by aqueous reaction with AgNO_3 .⁵⁷ In the bulk, Ag_2Se has an orthorhombic crystal structure at ambient conditions (Fig. 5B), and will transform to a super ionic cubic structure at 135 °C. As synthesized nanowires are in the room temperature equilibrium phase, which has an orthorhombic crystal structure. They can be converted to the high temperature super ionic cubic phase by heating, but do not fully transform until 180 °C. This cubic crystal structure can be stabilized all the way down to room temperature (Fig. 5C), far below the transition temperature, although in some nanowires the final structure after a temperature cycle is a mixture of the orthorhombic and cubic phases (Fig. 5G). A schematic of the observed process is shown in Fig. 5A, and a series of SAED images for a single nanowire transition is illustrated in panels D–

G. The phase change induced by temperature cycling is correlated with a huge change in electrical transport properties. As synthesized the nanowires with orthorhombic structure have ohmic conductivity, but after annealing at 180 °C they display a volatile threshold switching similar to that observed in metal chalcogenide glasses,⁵⁵ further evidence for a chemical disordering of the cation sublattice.

Physical transformations in nanowires have already found applications.^{44,58} Nonvolatile memory is receiving a great deal of interest as a replacement for flash memory is sought. The current leading technology is phase change memory (PCM). PCM operates by driving a small volume of material through a reversible crystal-amorphous structural transition (Fig. 6A). The phase-change is actuated electrically by joule heating, and the two states can be easily distinguished due to the substantially lower resistivity of the crystalline phase compared to the amorphous one. PCM nanowires (NWs) developed recently by our group⁴² and others^{40,41,46} offer new candidates to be used as the active material switching devices (Fig. 7A). NWs present several advantages over patterned thin films: they have smooth well-defined surfaces, they are initially in a high quality single crystalline state, and they can be deposited on a substrate in a single solvent free room temperature step.⁵⁹ The electrical switching properties of single NWs have been studied and excellent scaling behaviors have been shown (Fig. 6B).^{40,60}

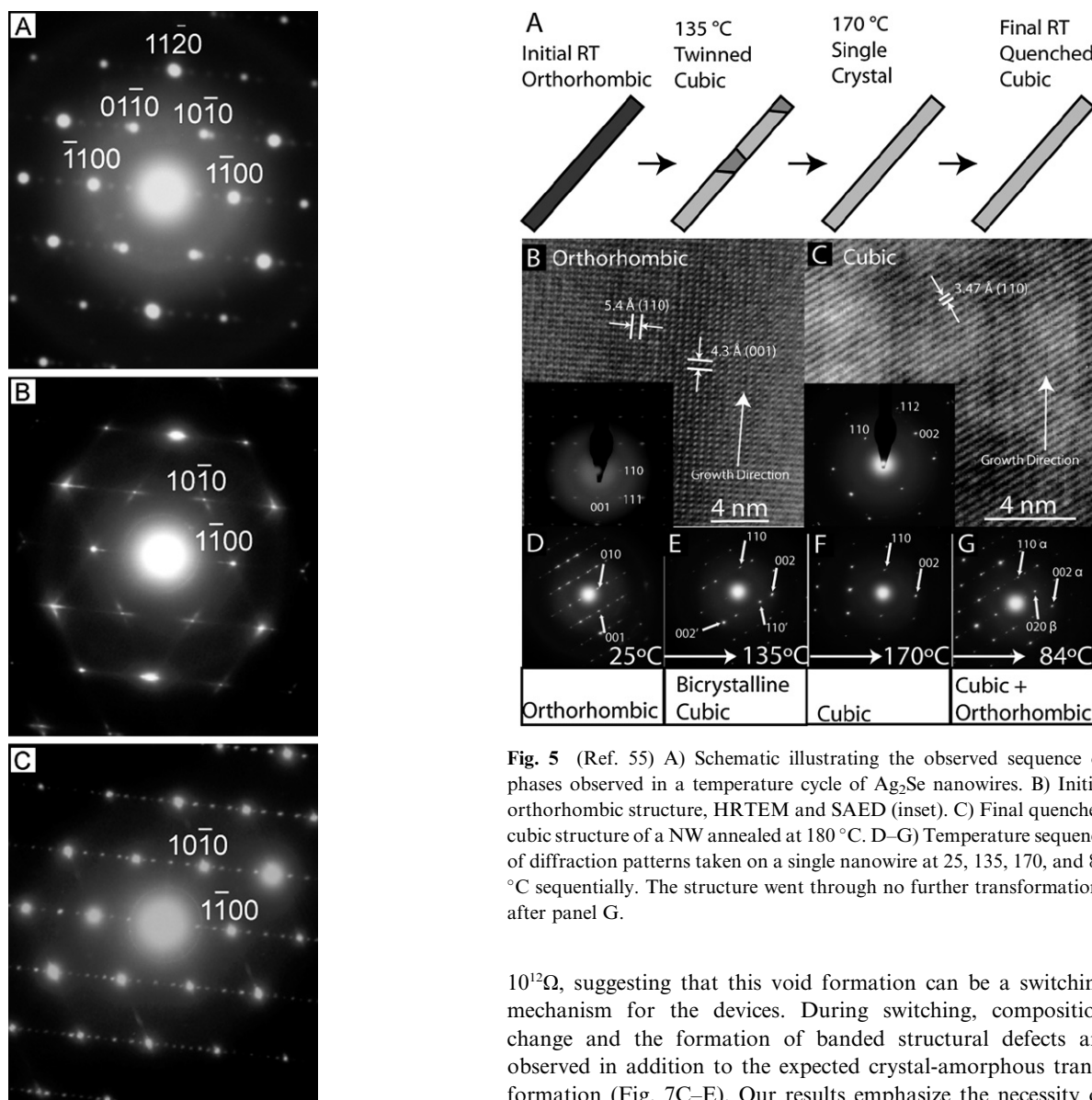


Fig. 4 (Ref. 52) A–C) SAED patterns of the In₂Se₃ NW recorded at 22, 267, and 23 °C, sequentially.

Recently we have combined single PCM nanowire device with ex-situ and in-situ transmission electron microscopy to correlate directly nanoscale structural transformations with electrical switching.⁶¹ We have discovered surprising new results. Instead of crystalline-amorphous transformation, the dominant switching mechanism during multiple cycling appears to be the opening and closing of voids in the nanowires due to material migration, which offers a new mechanism for memory. Fig. 7B shows a GeTe nanowire device after a 10V pulse in air, which resulted in a current of approximately 1.3mA, the two-probe resistance was changed to $10^{12} \Omega$. Interestingly, a dramatic structural change was observed close to one of the contacts (bright contrast in NW). The structure observed is a thin amorphous hollow tube of GeO_x confirmed by EDS, indicating a void formed in the NW. GeO_x is highly resistive and even a small segment close to the metal contact can increase the measured NW resistance up to

Fig. 5 (Ref. 55) A) Schematic illustrating the observed sequence of phases observed in a temperature cycle of Ag₂Se nanowires. B) Initial orthorhombic structure, HRTEM and SAED (inset). C) Final quenched cubic structure of a NW annealed at 180 °C. D–G) Temperature sequence of diffraction patterns taken on a single nanowire at 25, 135, 170, and 84 °C sequentially. The structure went through no further transformations after panel G.

$10^{12} \Omega$, suggesting that this void formation can be a switching mechanism for the devices. During switching, composition change and the formation of banded structural defects are observed in addition to the expected crystal-amorphous transformation (Fig. 7C–E). Our results emphasize the necessity of direct correlation of structure with phase transformation.

Chemical transformations in 1D

Chemical transformation of solid-state materials is an important approach for new materials synthesis based on existing materials and is critical for understanding multiple-step materials and device processing. Chemical transformations in one-dimensional nanostructures have been extensively explored, primarily as a route to extend the number of structures which can be synthesized.⁶² Many of the unique behaviors observed in zero-dimensional structures, such as single crystal to single crystal transformations by ion exchange⁵ and the creation of hollow nanostructures by the nanoscale Kirkendall⁶³ effect, have been observed. Unlike the zero-dimensional case, the role of strain and the existence of multiple domains in a single one-dimensional nanostructure can lead to surprising results. In the partial chemical conversion of CdSe nanorods to Ag₂Se, for instance, it has been found that the strain caused by domain formation leads

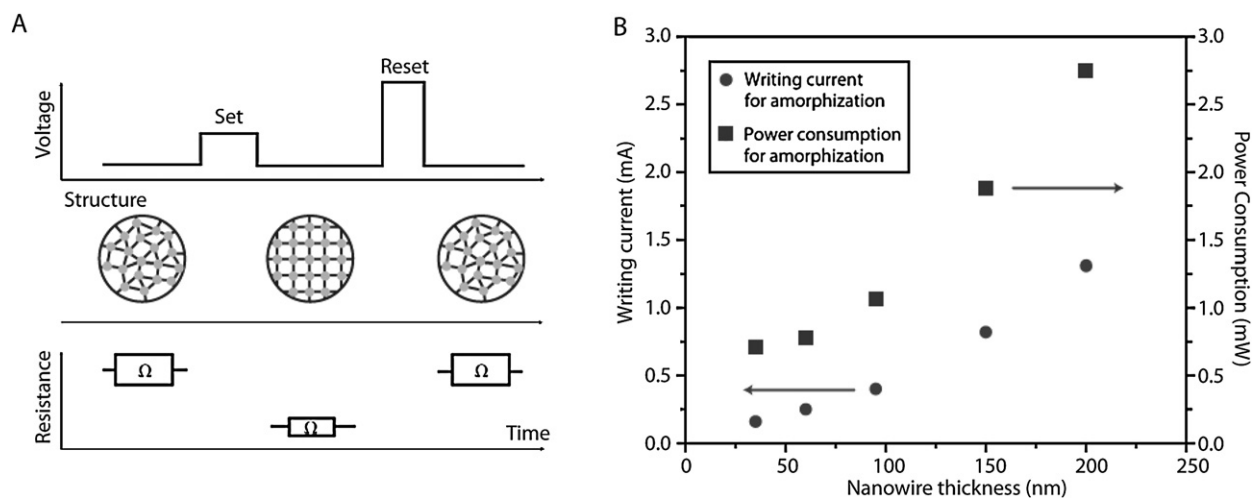


Fig. 6 A) Schematic of operation for a phase change memory device.⁶⁴ B) Observed scaling behavior of writing current and power consumption for the “reset” step of device operation with nanowire diameter in single nanowire GeTe devices.⁵⁸

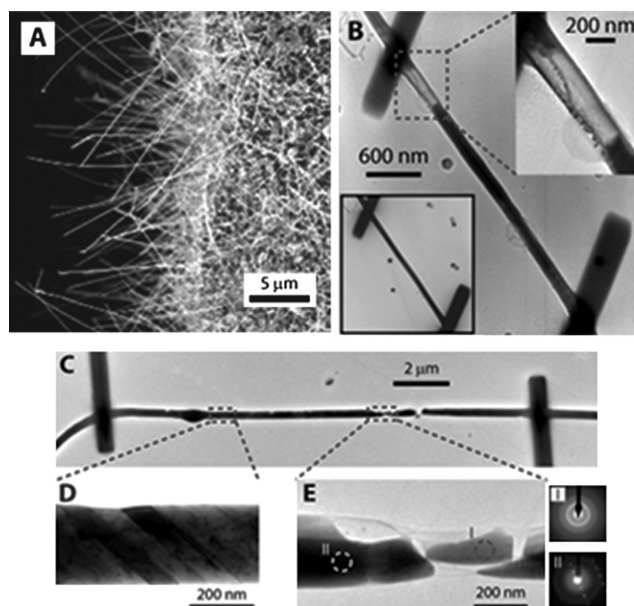


Fig. 7 (Ref. 61) A) GeTe nanowires grown by the vapor-liquid-solid technique. B) A single nanowire device after being subjected to a 10 V pulse. There is a void formed near one contact (upper inset). No void was observed prior to pulsing (lower inset). C) Another NW after a low magnitude voltage pulse. This NW exhibits the formation of a banded structure D), as well as void formation and amorphization E).

to the spontaneous creation of a one-dimensional superlattice of Ag_2Se and CdSe domains.⁶⁵

One materials system we investigate is CuInSe_2 , which has received a great deal of interest recently for its application to energy conversion.^{66,67} Due to its exceptionally high adsorptivity and direct band gap of ~ 1 eV, CuInSe_2 is one of the leading materials for thin film photovoltaics. In a heterojunction with CdS and when doped with Ga, polycrystalline $\text{Cu}(\text{In,Ga})\text{Se}_2$ solar cells have reached nearly 20% conversion efficiencies,⁶⁶ the record for polycrystalline solar cells. The record setting solar cells are fabricated in a complicated 3 step coevaporation process

which involves several high temperature annealing steps. Their behavior is still poorly understood, since the grain boundaries do not seem to lead to significant recombination as would be expected in most materials systems. There have been several attempts to explain this unexpected behavior,^{68–70} and while they disagree on many points there is a growing consensus it must be due to some sort of chemical inhomogeneity formed in the active layer or at the CdS-CuInSe_2 junction. Due to the very high adsorptivity of CuInSe_2 most of the photons are adsorbed within the first 200 nm of the film, so the structure of the interface with the CdS is of critical importance.

In order to study this interface, we have fabricated nanoscale heterojunctions of CdS and CuInSe_2 starting with VLS grown CuInSe_2 nanowires.⁷¹ CdS was deposited onto the CuInSe_2 nanowires in a chemical bath deposition process (CBD) which is the most common processing route in thin film solar cells. Given the tendency in other nanoscale systems for cation exchange reactions to occur rapidly one might expect some change in the CuInSe_2 during the process. This is in fact observed by TEM examination of the nanowires at each point in the process. Fig. 8 illustrates the structure of this system with time. Within short times, a thin CdS film is formed and depletion of Cu by its diffusion from CuInSe_2 into the CdS can be observed, which has the effect of creating a superlattice structure in the CIS nanowire near the interface. As in In_2Se_3 , this structure is generated by the ordering of vacancies, in this case copper vacancies, in the now substoichiometric CIS nanowire. At longer times, as would be expected from the nanoscale Kirkendall effect, hollow structures of uniform composition are observed (Fig. 8). These results give fundamental understanding of chemical transformations taking place during materials processing and provide guidance for solar cell fabrication.

Electrochemical transformations in 1D

Electrochemical transformation is a concerted process involving electrical current, ionic motion and/or chemical transformation, whose efficiency is critical for energy storage devices such as batteries, supercapacitors and fuel cells. One-dimensional

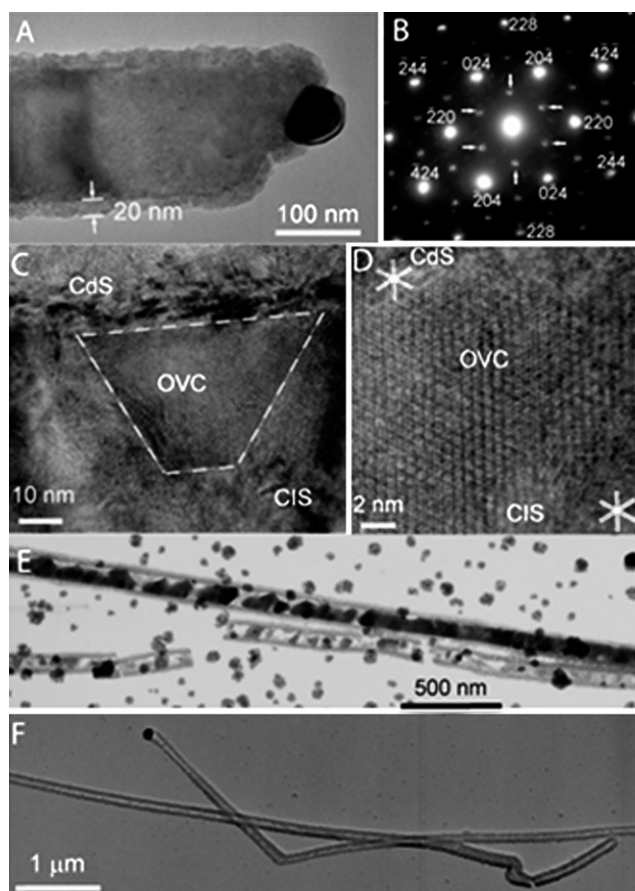


Fig. 8 (Ref. 71) A) CuInSe_2 nanowire with a 20 nm CdS shell deposited by chemical bath deposition (CBD). B) Diffraction pattern of nanowire in A showing the CdS is deposited epitaxially on the underlying nanowire. C) Ordered vacancy structure observed near the CdS interface with longer CBD time. D) HRTEM of structure in C. E) TEM image of nanowire with longer CBD time showing the formation of voids. F) TEM of nanowire after a long CBD showing a hollow structure.

materials can provide a unique opportunity to engineer electrochemical devices to have improved electronic and ionic motion as well as electrochemical transformations. There are several properties of nanowires that can allow for these improvements to be realized. First, the one-dimensional structure of the nanowires can allow for efficient electron transport along the length of each nanowire. This is an advantage over nanoparticles, where charge carriers must rely on inter-particle transport. Also, often conducting additives and a polymeric binder must be used in the case of particle films to allow for good electron transport and maintain a cohesive structure. In contrast, since nanowires can be synthesized on a conducting substrate, good contact between each nanowire and the source of electrons can be made, eliminating the need for conductive additives. Second, the small nanoscale diameters of the nanowires means that the distance required for ionic transport can be very small. Combined with the large surface area of the nanowires, the ionic flux inside the material can be quite large. Third, the small size of the nanowires means that mechanical strain can be easily relaxed during electrochemical transformations, which often involve a concerted phase change or volume change that is crucial to the performance

of the material. For example, large volume changes in lithium-containing alloys can result in pulverization of the material and loss of electrical contact (Fig. 9A). By using nanowires, the large volume changes can be accommodated without pulverization (Fig. 9B). Thus, by using nanowires, the kinetic barrier of transformation is reduced and moreover the mechanical and electrical integrity of the whole device is maintained. Our group has explored the unique properties of nanowires as high performance lithium-ion battery electrodes. We will discuss two examples here. One example is the application of Si and Ge nanowires for a new type of high capacity anodes.^{39,72} The other example is the use of LiMn_2O_4 nanorods for a new type of cathode with high power capabilities.⁷³

There has been much research interest in the development of higher specific energy lithium batteries for applications such as portable electronic devices, electric vehicles, and implantable medical devices.⁷⁴ One direction being pursued is the investigation of alternatives for the Li-graphite anode, which can incorporate one Li per six carbon atoms (LiC_6) to give a maximum theoretical specific capacity of 372 mAh/g. A number of metal and metal-metalloid materials have been known for some time to react with large amounts of Li,⁷⁵ and therefore may be the basis for high capacity electrodes. For example, the incorporation of 4.4 Li atoms per Si or Ge gives the extremely high specific capacity of 4200 or 1600 mAh/g. The relatively low discharge potential of these Si-Li and Ge-Li alloys makes them attractive as anode materials. However, the large inherent change in specific volume (up to about 300%) during the insertion and extraction of large amounts of Li causes pulverization and a loss of electrical contact between the active material and the current collector. The result is a reduction in the effective capacity during cycling. Previous studies⁷⁶⁻⁷⁹ on Si bulk films and micron-sized particles have shown capacity fading and short battery lifetime due to pulverization and loss of electrical contact (Fig. 9C, triangles). We have fabricated our novel Si or Ge nanowire anodes to overcome these problems. The structure of our nanowire anode configuration is shown schematically in Fig. 9B. Nanowires are grown directly on the metallic current collector substrate. In addition to the advantages of the large surface area and short Li diffusion distance in the NWs, this geometry allows for better accommodation of the large inherent volume changes without the initiation of fracture and also allows for efficient electron transport. In addition, since every nanowire is connected to the current-carrying electrode, the need for binders or conducting additives is eliminated.

Using the nanowire electrode design, we have been able to charge/discharge electrodes for a large number of cycles with much higher capacities than graphite (Fig. 9C and D). Excitingly, the SiNWs displayed capacities 10 times greater than graphite and even also showed improved capacities over Si nanocrystals,⁷⁶ confirming that the advantages of our nanowire geometry can indeed be translated into improved device performance.

The important transformation in a Si or Ge nanowire electrode is the crystalline-amorphous transformation. During the first charging cycle, lithium ions are inserted into the nanowire in a process that converts the single-crystalline material into an amorphous Li-alloy that has a larger volume. We have used X-ray diffraction and transmission electron microscopy to follow this process (Fig. 10). The crystalline-amorphous transformation

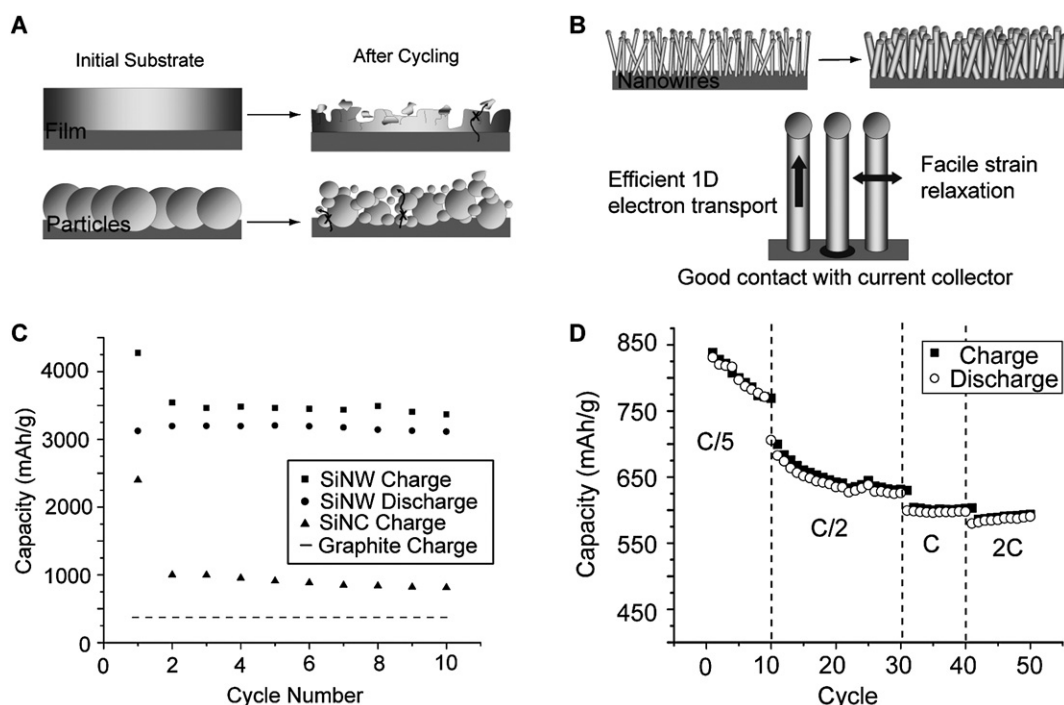


Fig. 9 A)³⁹ The volume of silicon anodes changes by about 400% during electrochemical cycling. As a result, Si films and particles tend to pulverize during cycling. Much of the material loses contact with the current collector, resulting in poor transport of electrons, as indicated by the arrow. B)³⁹ NWs grown directly on the current collector do not pulverize or break into smaller particles after cycling. Rather, facile strain relaxation in the NWs allows them to increase in diameter and length without breaking. This NW anode design has each NW connecting with the current collector, allowing for efficient 1D electron transport down the length of every NW. C)³⁹ Capacity versus cycle number for the Si NWs at the C/20 rate (current needed for 20h discharge). The charge data for Si nanocrystals (triangles) and the theoretical capacity for lithiated graphite (dashed line) are shown as a comparison to show the improvement when using Si NWs. D)⁷² Capacity versus cycle number for the GeNWs at the C/20 rate showing a capacity more than 3× higher than for graphite.

takes place in steps starting with the single-crystalline nanowire, then coexistence of a crystalline-amorphous phase in the same nanowire, to a complete amorphous phase throughout the entire nanowire. This is illustrated in Fig. 10A–B, with the Si crystalline reflections disappearing in the XRD and SAED patterns with increased lithiation. The high resolution TEM images also clearly show the gradual transformation into the amorphous Li-alloy. We found that both the nanowire diameter and length are increased significantly, resulting in a large volume expansion. Fig. 10C shows the SEM images of the Si and GeNWs, respectively, before and after lithiation. The exciting finding is that nanowires do not break during the drastic transformation, which is the key reason for the high performance of these nanowire electrodes.

For lithium-ion battery cathodes, Li_xCoO_2 is a commonly used material in commercial batteries and has a charge capacity of 140 mAh/g with a practical value of x from 0.5 to 1. However, the high cost, toxicity and limited abundance of cobalt have been recognized to be disadvantageous. One alternative promising candidate is the spinel LiMn_2O_4 , which has a theoretical charge storage capacity of 148 mAh/g. Spinel LiMn_2O_4 is advantageous due to its low cost, environmental friendliness, and high abundance. The structural transformation during charge and discharge in the potential range of 3.5 to 4.3V involves two nearly identical cubic phases of LiMn_2O_4 that have a small difference in lattice parameter. We recently synthesized and studied nanorods

of LiMn_2O_4 . Compared with micrometer sized, commercially available powders, the nanorods show a higher charge storage capacity at high power rates (Fig. 11).⁷³ The better performance of the nanorods can be attributed to fast kinetics resulting from their facile strain relaxation and large surface to volume ratio.

Summary and outlook

Nanoscale transformation is a rich and exciting field of research with many potentially exciting implications for a wide array of technologies. The fundamental study of transformations induced by changes in temperature, pressure, and chemical composition has been well developed for 0-dimensional particles and many important thermodynamic, kinetic, and mechanistic differences have been identified between these systems and the bulk. Some of this work has already been extended to 1-dimensional systems, which show many of the same exciting behaviors, but also offer a much easier path to device integration which allows for these unique behaviors to be utilized in a variety of technologies.

The central goals for this field going forward should be to identify which of the nanoscale transformation behaviors can be best utilized to improve the performance of actual devices. Several examples have been mentioned in this feature article, including novel synthesis pathways using defect free solid state structural transformations, lowered operation energy for phase change memory due to possible melting point depression, and

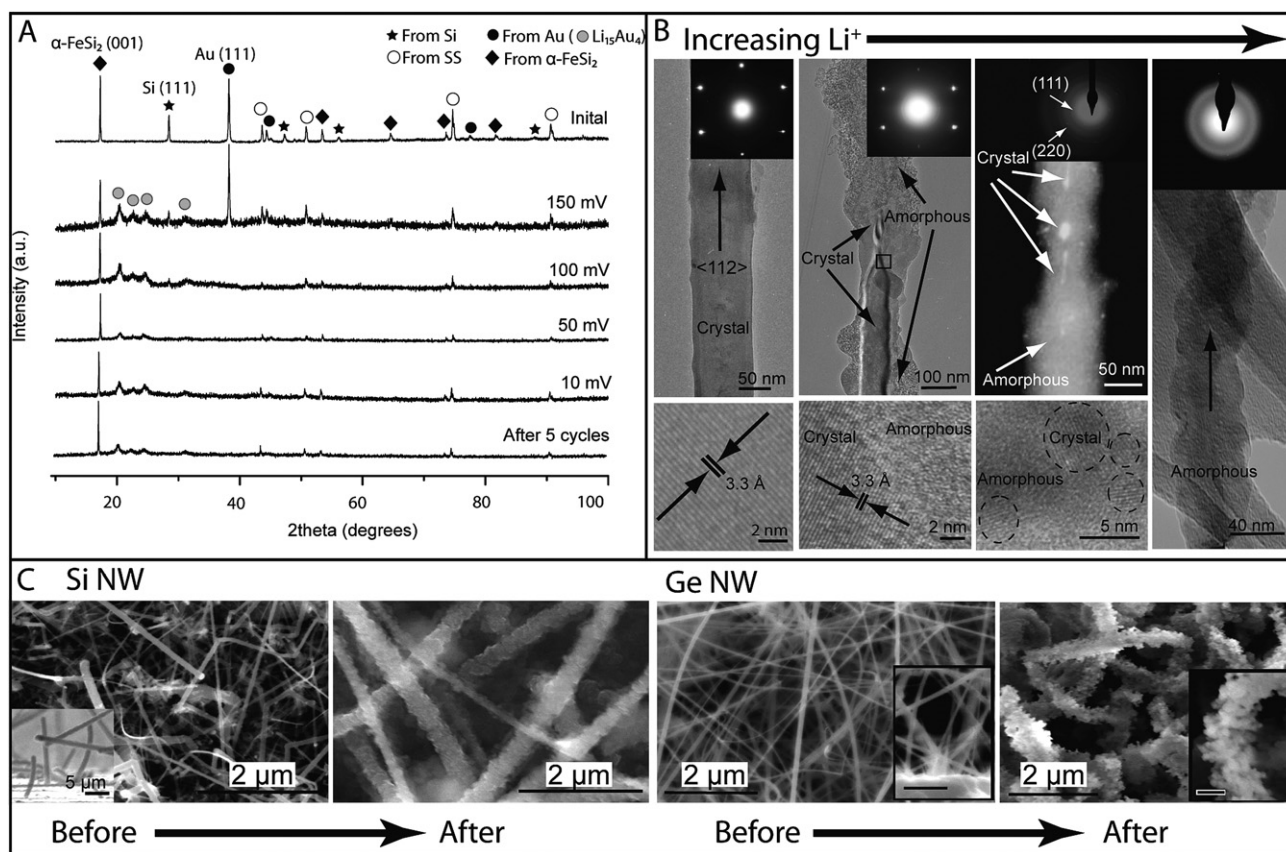


Fig. 10 A) ^{39}Si XRD patterns of Si NWs before electrochemical cycling (initial) and at different potentials during the first charge. As the potential is lowered, more lithiation occurs and the Si reflections disappear, indicating that the Si NWs become amorphous. After five cycles, the XRD pattern did not show any crystalline peaks, suggesting that the Si NWs remain amorphous and no recrystallization occurs even after Li is fully removed. B) ^{39}Si From right to left, with increasing lithiation: TEM data for Si NWs at different stages of the first charge; a single-crystalline, pristine Si NW before electrochemical cycling. The SAED spots (inset) and HRTEM lattice fringes (bottom) are from the Si 1/3(224) planes; NW charged to 100 mV showing a Si crystalline core and the beginning of the formation of a Li_xSi amorphous shell. The HREM (bottom) shows an enlarged view of the region inside the box; dark-field image of a NW charged to 50 mV showing an amorphous Li_xSi wire with crystalline Si grains (bright regions) in the core. The spotty rings in the SAED (inset) are from crystalline Si. The HRTEM (bottom) shows some Si crystal grains embedded in the amorphous wire; a NW charged to 10 mV is completely amorphous $\text{Li}_{4.4}\text{Si}$. The SAED (top) shows diffuse rings characteristic of an amorphous material. C) ^{39}Si SEM images of pristine Si NWs before (right) and after (left) electrochemical cycling (same magnification). The inset in the left image is a cross-sectional image showing that the NWs are directly contacting the stainless steel current collector. D) ^{39}Si Right: SEM image of as-grown GeNWs on SS. Inset, cross-sectional view (scale bar, 500 nm). Left: SEM image of GeNWs on SS after Li cycling. The magnification is the same as that in Fig. 3a. Inset, zoomed-in view of a textured NW (scale bar, 250 nm).

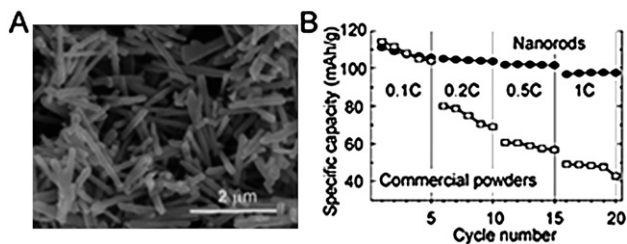


Fig. 11 (Ref. 73) A) As-synthesized spinel LiMn_2O_4 nanorods with typical diameter of 130 nm and length of 1.2 μm . B) Discharge specific capacity curve vs. number of cycles for nanorods (black dots) and commercial powder electrode (white squares) at different power rates (1C = 148 mAh/g).

high capacity lithium ion batteries based on nanomaterial's ability to undergo large volume changes during transformation without fracture. Due to the large hysteresis observed in a variety

of solid state structural transitions it may also be possible to quench desirable phases from high temperatures or pressures to ambient conditions where in the bulk this would be impossible.

In addition to the choice of appropriate technological problems, more work needs to be done to address specifically the size dependence of these behaviors. Synthesis of one-dimensional structures continues to improve both in morphology control and in terms of flexibility for materials choice; however, the degree of size control which has been achieved for nanocrystals has yet to be duplicated. One should expect many of the trends which have been observed in nanocrystals to also appear in nanowires, but in order to rigorously explore the differences between 0- and 1-dimensional systems it will be necessary to in large part duplicate much of the careful work which has been done for nanocrystals in nanowires. This will require the ability to synthesize or fabricate nanowires with well controlled and homogeneous diameters, which is still possible only in a handful of systems.

However, if this can be achieved there is significant potential for both exciting scientific discoveries and unanticipated technological application.

References

- 1 P. Buffat and J. P. Borel, *Physical review. A*, 1976, **13**, 2287–2298.
- 2 C. Coombes, *Journal of physics. F, Metal physics*, 1972, **2**, 441.
- 3 A. Goldstein, C. M. Echer and A. P. Alivisatos, *Science*, 1992, **256**, 1425–1427.
- 4 S. H. Tolbert and A. P. Alivisatos, *Annu. Rev. Phys. Chem.*, 1995, **46**, 595–625.
- 5 D. Son, S. M. Hughes, Y. D. Yin and A. P. Alivisatos, *Science*, 2004, **306**, 1009–1012.
- 6 A. S. Arico, P. Bruce, B. Scrosati, J. M. Tarascon and W. Van Schalkwijk, *Nature materials*, 2005, **4**, 366–377.
- 7 A. Manthiram, A. V. Murugan, A. Sarkar and T. Muraliganth, *Energy Environ. Sci.*, 2008, DOI: 10.1039/b811802g.
- 8 P. X. Gao, Y. Ding, W. J. Mai, W. L. Hughes, C. S. Lao and Z. L. Wang, *Science*, 2005, **309**, 1700–1704.
- 9 S. Meister, H. L. Peng, K. McIlwrath, K. Jarausch, X. F. Zhang and Y. Cui, *Nano Letters*, 2006, **6**, 1514–1517.
- 10 J. Zhu, H. L. Peng, A. F. Marshall, D. M. Barnett, W. D. Nix and Y. Cui, *Nature Nanotechnology*, 2008, **3**, 477–481.
- 11 M. Law, J. Goldberger and P. D. Yang, *Annual Review of Materials Research*, 2004, **34**, 83–122.
- 12 R. H. Baughman, C. X. Cui, A. A. Zakhidov, Z. Iqbal, J. N. Barisci, G. M. Spinks, G. G. Wallace, A. Mazzoldi, D. De Rossi, A. G. Rinzler, O. Jaschinski, S. Roth and M. Kertesz, *Science*, 1999, **284**, 1340–1344.
- 13 H. Zheng, J. Wang, S. E. Lofland, Z. Ma, L. Mohaddes-Ardabili, T. Zhao, L. Salamanca-Riba, S. R. Shinde, S. B. Ogale, F. Bai, D. Viehland, Y. Jia, D. G. Schlom, M. Wuttig, A. Roytburd and R. Ramesh, *Science*, 2004, **303**, 661–663.
- 14 D. L. Leslie-Pelecky and R. D. Rieke, *Chem. Mat.*, 1996, **8**, 1770–1783.
- 15 H. Chandrasekaran, G. U. Sumanasekara and M. K. Sunkara, *J. Phys. Chem. B*, 2006, **110**, 18351–18357.
- 16 M. Kuno, *Phys. Chem. Chem. Phys.*, 2008, **10**, 620–639.
- 17 N. Wang, Y. Cai and R. Q. Zhang, *Mater. Sci. Eng. R-Rep.*, 2008, **60**, 1–51.
- 18 P. Pawlow, *Zeitschrift Fur Physikalische Chemie–Stochiometrie Und Verwandtschaftslehre*, 1909, **65**, 545–548.
- 19 C. A. M. Blackman *Structure and Properties of Thin Films*, Wiley, New York, 1959.
- 20 H. Peng, C. Xie, D. T. Schoen and Y. Cui, *Nano Lett.*, 2008, **8**, 1511–1516.
- 21 S. Clark, S. G. Prilliman, C. K. Erdonmez and A. P. Alivisatos, *Nanotechnology*, 2005, **16**, 2813–2818.
- 22 Q. Guo, Y. Zhao, W. L. Mao, Z. Wang, Y. Xiong and Y. N. Xia, *Nano Lett.*, 2008, **8**, 972–975.
- 23 K. Jacobs, D. Zaziski, E. C. Scher, A. B. Herhold and A. P. Alivisatos, *Science*, 2001, **293**, 1803–1806.
- 24 S. Tolbert and A. P. Alivisatos, *Science*, 1994, **265**, 373–376.
- 25 S. Tolbert and A. P. Alivisatos, *The Journal of chemical physics*, 1995, **102**, 4642–4656.
- 26 S. Li, Z. Wen and Q. Jiang, *Scr. Mater.*, 2008, **59**, 526–529.
- 27 Y. D. Yin, R. M. Rioux, C. K. Erdonmez, S. Hughes, G. A. Somorjai and A. P. Alivisatos, *Science*, 2004, **304**, 711–714.
- 28 Y. Cui, Z. H. Zhong, D. L. Wang, W. U. Wang and C. M. Lieber, *Nano Lett.*, 2003, **3**, 149–152.
- 29 Y. Chen, G. Y. Jung, D. A. A. Ohlberg, X. M. Li, D. R. Stewart, J. O. Jeppesen, K. A. Nielsen, J. F. Stoddart and R. S. Williams, *Nanotechnology*, 2003, **14**, 462–468.
- 30 C. Fash, A. Fuhrer, M. T. Bjork and L. Samuelson, *Nano Lett.*, 2005, **5**, 1487–1490.
- 31 N. A. Melosh, A. Boukai, F. Diana, B. Gerardot, A. Badolato, P. M. Petroff and J. R. Heath, *Science*, 2003, **300**, 112–115.
- 32 M. H. Huang, S. Mao, H. Feick, H. Q. Yan, Y. Y. Wu, H. Kind, E. Weber, R. Russo and P. D. Yang, *Science*, 2001, **292**, 1897–1899.
- 33 Y. Cui, Q. Q. Wei, H. K. Park and C. M. Lieber, *Science*, 2001, **293**, 1289–1292.
- 34 B. Sun, M.E. and N. C. Greenham, *Nano Lett.*, 2003, **3**, 961–963.
- 35 W. U. Huynh, J. J. Dittmer and A. P. Alivisatos, *Science*, 2002, **295**, 2425–2427.
- 36 A. I. Boukai, Y. Bunimovich, J. Tahir-Kheli, J. K. Yu, W. A. Goddard and J. R. Heath, *Nature*, 2008, **451**, 168–171.
- 37 A. I. Hochbaum, R. K. Chen, R. D. Delgado, W. J. Liang, E. C. Garnett, M. Najarian, A. Majumdar and P. D. Yang, *Nature*, 2008, **451**, 163–U165.
- 38 X. D. Wang, J. H. Song, J. Liu and Z. L. Wang, *Science*, 2007, **316**, 102–105.
- 39 C. Chan, H. Peng, G. Liu, K. McIlwrath, X. F. Zhang, R. A. Huggins and Y. Cui, *Nature nanotechnology*, 2008, **3**, 31–35.
- 40 S. H. Lee, Y. Jung and R. Agarwal, *Nature Nanotechnology*, 2007, **2**, 626–630.
- 41 D. Yu, J. Wu, Q. Gu and H. Park, *Journal of the American Chemical Society*, 2006, **128**, 8148–8149.
- 42 S. Meister, H. Peng, K. McIlwrath, K. Jarausch, X. F. Zhang and Y. Cui, *Nano Letters*, 2006, **6**, 1514–1517.
- 43 J. Q. Wu, Q. Gu, B. S. Guiton, N. P. de Leon, O. Y. Lian and H. Park, *Nano Lett.*, 2006, **6**, 2313–2317.
- 44 Q. Gu, A. Falk, J. Q. Wu, O. Y. Lian and H. K. Park, *Nano Lett.*, 2007, **7**, 363–366.
- 45 Y. C. Chou, W. W. Wu, S. L. Cheng, B. Y. Yoo, N. Myung, L. J. Chen and K. N. Tu, *Nano Lett.*, 2008, **8**, 2194–2199.
- 46 J. S. Lee, S. Brittman, D. Yu and H. Park, *Journal of the American Chemical Society*, 2008, **130**, 6252–6258.
- 47 X. W. Wang, G. T. Fei, K. Zheng, Z. Jin and L. De Zhang, *Appl. Phys. Lett.*, 2006, **88**.
- 48 X. W. Wang, G. T. Fei, B. Wang, M. Wang, K. Zheng, Z. Jin and L. De Zhang, *Appl. Phys. Lett.*, 2007, **91**.
- 49 G. K. Goswami and K. K. Nanda, *Appl. Phys. Lett.*, 2007, **91**.
- 50 K. B. Lee, S. M. Lee and J. Cheon, *Advanced Materials*, 2001, **13**, 517.
- 51 M. E. Toimil-Molares, A. G. Balogh, T. W. Cornelius, R. Neumann and C. Trautmann, *Appl. Phys. Lett.*, 2004, **85**, 5337–5339.
- 52 H. Peng, D. T. Schoen, S. Meister, X. F. Zhang and Y. Cui, *J. Am. Chem. Soc.*, 2007, **129**, 34–35.
- 53 J. Vanlanduyt, G. Vantendelo and S. Amelinckx, *Phys. Status Solidi A- Appl. Res.*, 1975, **30**, 299–314.
- 54 C. S. Sunandana and P. S. Kumar, *Bulletin of Materials Science*, 2004, **27**, 1–17.
- 55 D. T. Schoen, C. Xie and Y. Cui, *J. Am. Chem. Soc.*, 2007, **129**, 4116.
- 56 B. Gates, B. Mayers, B. Cattle and Y. N. Xia, *Advanced Functional Materials*, 2002, **12**, 219–227.
- 57 B. Gates, Y. Y. Wu, Y. D. Yin, P. D. Yang and Y. N. Xia, *J. Am. Chem. Soc.*, 2001, **123**, 11500–11501.
- 58 S. H. Lee, Y. Jung and R. Agarwal, *Nature nanotechnology*, 2007, **2**, 626–630.
- 59 T. O. Sedgwick, B. J. Agule and A. N. Broers, *Journal of the Electrochemical Society*, 1972, **119**, 1769.
- 60 S. H. Lee, D. K. Ko, Y. Jung and R. Agarwal, *Applied Physics Letters*, 2006, **89**.
- 61 S. Meister, D. T. Schoen, M. Topinka, A. Minor and Y. Cui, *Nano Lett.*, 2008, DOI: 10.1021/nl802808f.
- 62 U. Jeong, P. H. C. Camargo, Y. H. Lee and Y. N. Xia, *J. Mater. Chem.*, 2006, **16**, 3893–3897.
- 63 Y. Yin, R. M. Rioux, C. K. Erdonmez, S. M. Hughes, G. A. Somorjai and A. P. Alivisatos, *Science*, 2004, **304**, 711–714.
- 64 M. Wuttig, *Nature materials*, 2005, **4**, 265–266.
- 65 R. D. Robinson, B. Sadtler, D. O. Demchenko, C. K. Erdonmez, L. W. Wang and A. P. Alivisatos, *Science*, 2007, **317**, 355–358.
- 66 I. Repins, M. A. Contreras, B. Egaas, C. DeHart, J. Scharf, C. L. Perkins, B. To and R. Noufi, *Prog. Photovoltaics*, 2008, **16**, 235–239.
- 67 A. Goetzberger, C. Hebling and H. W. Schock, *Mater. Sci. Eng. R-Rep.*, 2003, **40**, 1–46.
- 68 A. Zunger, *Thin Solid Films*, 2007, **515**, 6160–6162.
- 69 Y. Yan, R. Noufi and M. M. Al-Jassim, *Phys. Rev. Lett.*, 2006, **96**.
- 70 Y. Yan, C. S. Jiang, R. Noufi, S. H. Wei, H. R. Moutinho and M. M. Al-Jassim, *Phys. Rev. Lett.*, 2007, **99**.
- 71 H. Peng, C. Xie, D. T. Schoen, K. McIlwrath, X. F. Zhang and Y. Cui, *Nano Lett.*, 2007, **7**, 3734–3738.
- 72 C. K. Chan, X. F. Zhang and Y. Cui, *Nano Lett.*, 2008, **8**, 307–309.
- 73 D. K. Kim, P. Muralidharan, H. K. Lee, R. Ruffo, Y. Yang, C. Chan, H. Peng, R. A. Huggins and Y. Cui, *Nano Lett.*, 2008, DOI: 10.1021/nl8024328.
- 74 G. A. Nazri and G. Pistoia, *Lithium Batteries: Science and Technology*, Kluwer Academic/Plenum, Boston, 2004.
- 75 R. A. Huggins, 1999, pp. 13–19.

-
- 76 J. Graetz, C. C. Ahn, R. Yazami and B. Fultz, *Electrochemical and Solid State Letters*, 2003, **6**, A194–A197.
- 77 M. Green, E. Fielder, B. Scrosati, M. Wachtler and J. S. Moreno, *Electrochemical and Solid State Letters*, 2003, **6**, A75–A79.
- 78 U. Kasavajjula, C. S. Wang and A. J. Appleby, *Journal of Power Sources*, 2007, **163**, 1003–1039.
- 79 J. H. Ryu, J. W. Kim, Y. E. Sung and S. M. Oh, *Electrochemical and Solid State Letters*, 2004, **7**, A306–A309.